RESEARCH ON Z-SOURCE INVERTER CONTROL BASED ON STATE SPACE MODEL

Chaoda CHEN[1], Shaofang WU[2,*], Haocong CHEN[3], Yage WANG[4], Yayuan LUO[5], Junxian XIE[6]

To solve the low energy efficiency and inverter dead zone of the electrochemical power supply, we propose a new control method that uses a Z-source inverter as the intermediate cascade. The two states of the state space model, shoot-through and non-shoot-through, are derived mathematically, and the steady-state equation and the transfer function of z-network capacitance-voltage are both obtained. The voltage boost control structure of the Z-source network is analyzed. The circuit transfer function is optimized by adjusting the gain and adding the series advance correction device. The result shows that amplitude-frequency and phase-frequency characteristics are improved. The simulation model of the Z-source inverter circuit is built. The simulation analysis shows that the closed-loop system has strong anti-interference ability, which can provide a stable and suitable voltage for the subsequent circuit. The control circuit of the Z-source inverter is designed, and the direct duty cycle D and M57962 driving circuits are tested in this paper. The results show that the duty cycle can be adjusted at 0-45% continuously, and the peak pulse of the driving circuit meets the requirements.

Keywords: state space model, Z-source inverter, controller optimization, simulation analysis

1. Introduction

The Z-Source inverter is a power converter topology proposed in 2003 by Peng Fangzheng at Michigan State University [1].The inverter of the Z-source can adjust the DC-link voltage and allow the shoot-through state [2-4]. Compared with the two-stage combination of inverter and transformer, the Z-source inverter can

[1] Associate Professor, School of Naval Architecture and Ocean Engineering, Guangzhou Maritime University, Guangzhou Guangdong, 510725, China
[2] Associate Professor, School of Naval Architecture and Ocean Engineering, Guangzhou Maritime University, Guangzhou Guangdong, 510725, China, corresponding author:
*E-mail: 28477850@qq.com
[3] Student, Dongguan Wanjiang Middle School, Dongguan Guangdong, 523058, China
[4] Lecturer, College of Mechanical and Electrical Engineering, Guangdong University of Science and Technology, Dongguan, 523000, China
[5] Student, School of Naval Architecture and Ocean Engineering, Guangzhou Maritime University, Guangzhou Guangdong, 510725, China
[6] Student, School of Naval Architecture and Ocean Engineering, Guangzhou Maritime University, Guangzhou Guangdong, 510725, China

make better use of power without loss due to the two-stage transformation [5-8].

The Z-network is added between the DC voltage source and the H-bridge of the Z-source inverter, which can form a new circuit characteristic. This characteristic allows both switches of the same bridge arm to be turned on simultaneously, which makes the Z-source inverter overcome the shortcomings of traditional inverters. The switch state of S_1-S_4 can be divided into two states: shoot-through and non-shoot-through. When S_1 and S_2 are connected simultaneously, or S_3 and S_4 are connected simultaneously, or S_1-S_4 are all connected simultaneously, the circuit forms a shoot-through state. In other cases, form a non-shoot-through state. H-bridge is short-circuited in the shoot-through state of the inverter bridge, and the DC-link voltage can be boosted in the non-shoot-through state to achieve the purpose of voltage rise. To quantitatively study the steady-state working state of the Z-source network, it is assumed that the inductance and capacitance parameters of the Z-source network are equal (L_1=L_2=L, C_1=C_2=C), which makes the Z-source network a symmetrical network [9-10].

2. State space model

The state space model is simple and clear, which is an effective model of a power electronic switch circuit. According to different switch states, Z-network can be divided into shoot-through and non-shoot-through, as shown in Fig. 1. Since the Z-source network has four energy storage units, the state equation derived from the model should be fourth order, and the DC power supply voltage V_D and load current I_O are both inputs [11]. The circuit parameters of the Z-source inverter are symmetrical and equal, that is L_1=L_2=L and C_1=C_2=C. The series equivalent resistance of inductance and capacitance is expressed by r and R respectively, and r_1=r_2, R1=R2.

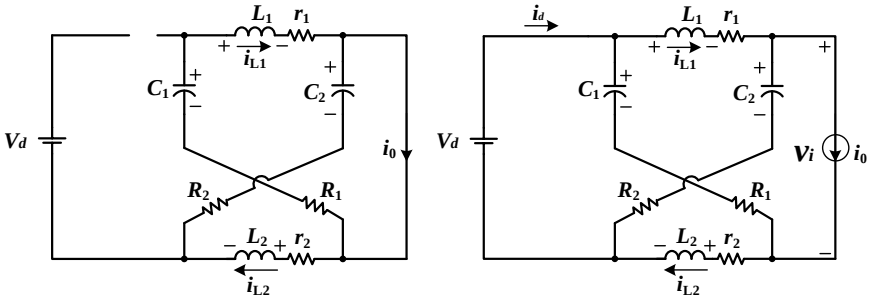

a) shoot-through b) non-shoot-through

Fig. 1. Two State Equivalent Circuit Diagrams of Networks

Fig. 1a) represents the shoot-through state, and the system state equation is shown in formula (1).

$$\frac{d}{dt}\begin{bmatrix} i_{L1} \\ i_{L2} \\ v_{C1} \\ v_{C2} \end{bmatrix} = A_1 \begin{bmatrix} i_{L1} \\ i_{L2} \\ v_{C1} \\ v_{C2} \end{bmatrix} + B_1 \begin{bmatrix} v_d \\ i_0 \end{bmatrix} \tag{1}$$

Among $A_1 = \begin{bmatrix} -\frac{R+r}{L} & 0 & \frac{1}{L} & 0 \\ 0 & -\frac{R+r}{L} & 0 & \frac{1}{L} \\ -\frac{1}{C} & 0 & 0 & 0 \\ 0 & -\frac{1}{C} & 0 & 0 \end{bmatrix}$, $B_1 = \begin{bmatrix} 0 & 0 \\ 0 & 0 \\ 0 & 0 \\ 0 & 0 \end{bmatrix}$.

Substituting A_1 and B_1 into formula (1), we can get $\frac{di_{L1}}{dt} = -\frac{R+r}{L} i_{L1} + (-\frac{1}{L}) i_{L1} + 0$.

It can be seen from the equivalent circuit of the shoot-through circuit that R_1, r_1, L_1 and C_1 constitute a loop.

According to Kirchhoff's theorem, we can get $U_{R_1} + U_{r_1} + U_{L_1} + U_{C_1} = 0$ (i_L=i_C).

So $\frac{i_{L_1} dt}{C} + L\frac{di_{L_1}}{dt} + (R+r) i_{L_1} = 0$, which means $\frac{d_{i_{L_1}}}{dt} = -\frac{R+r}{L} i_{L1} - \frac{1}{C} i_{L_1}$.

Fig.. 1b) represents the non-shoot-through state, and the system state equation is shown in formula (2).

$$\frac{d}{dt}\begin{bmatrix} i_{L1} \\ i_{L2} \\ v_{C1} \\ v_{C2} \end{bmatrix} = A_2 \begin{bmatrix} i_{L1} \\ i_{L2} \\ v_{C1} \\ v_{C2} \end{bmatrix} + B_2 \begin{bmatrix} v_d \\ i_0 \end{bmatrix} \tag{2}$$

Among $A_2 = \begin{bmatrix} -\frac{R+r}{L} & 0 & 0 & \frac{1}{L} \\ 0 & -\frac{R+r}{L} & \frac{1}{L} & 0 \\ 0 & \frac{1}{C} & 0 & 0 \\ \frac{1}{C} & 0 & 0 & 0 \end{bmatrix}$, $B_2 = \begin{bmatrix} \frac{1}{L} & \frac{R}{L} \\ \frac{1}{L} & \frac{R}{L} \\ 0 & -\frac{1}{C} \\ 0 & -\frac{1}{C} \end{bmatrix}$.

Assuming that the duty cycle of the shoot-through state is D, the duty cycle of the non-shoot-through state is 1-D, and formula (1) and formula (2) are weighted to obtain the average state equation of the system as shown in formula (3).

$$\frac{d}{dt}\begin{bmatrix} i_{L1} \\ i_{L2} \\ v_{C1} \\ v_{C2} \end{bmatrix} = A\begin{bmatrix} i_{L1} \\ i_{L2} \\ v_{C1} \\ v_{C2} \end{bmatrix} + B\begin{bmatrix} v_d \\ i_0 \end{bmatrix} \tag{3}$$

Among $A = DA_1 + (1-D)A_2 = \begin{bmatrix} -\frac{R+r}{L} & 0 & \frac{D}{L} & -\frac{1-D}{L} \\ 0 & -\frac{R+r}{L} & -\frac{1-D}{L} & \frac{D}{L} \\ -\frac{D}{C} & \frac{1-D}{C} & 0 & 0 \\ \frac{1-D}{C} & -\frac{D}{C} & 0 & 0 \end{bmatrix}$

$B = DB_1 + (1-D)B_2 = \begin{bmatrix} \frac{1-D}{L} & \frac{R(1-D)}{L} \\ \frac{1-D}{L} & \frac{R(1-D)}{L} \\ 0 & -\frac{1-D}{C} \\ 0 & -\frac{1-D}{C} \end{bmatrix}$.

Formula (3) is the large signal model of the system. When the value on the left side of the formula is zero, the steady-state equation of the system can be obtained as shown in formula (4).

$$0 = A\begin{bmatrix} I_{L1} \\ I_{L2} \\ V_{C1} \\ V_{C2} \end{bmatrix} + B\begin{bmatrix} V_d \\ I_0 \end{bmatrix} \tag{4}$$

According to the symmetry of circuit parameters, $I_{L1}=I_{L2}=I_L$, $V_{C1}=V_{C2}=V_C$. When the equivalent series resistance of inductance and capacitance is ignored, V_C and I_L can be obtained from formula (4), as shown in formula (5) and formula (6).

$$V_C = \frac{1-D}{1-2D}V_d \tag{5}$$

$$I_L = \frac{1-D}{1-2D}I_0 \tag{6}$$

The dynamic model of the system is established by the disturbance method, and the static variable with disturbance is used to replace the variable in formula (3).

We can get $i_{L1} = I_L + \hat{i}_{L1}$, $i_{L2} = I_L + \hat{i}_{L2}$, $v_{C1} = V_C + \hat{v}_{C1}$, $v_{21} = V_C + \hat{v}_{C2}$, $v_d = V_d + \hat{v}_d$, $i_0 = I_0 + \hat{i}_0$.

Ignore the higher-order term of the small signal, as shown in formula (7) after finishing.

$$\frac{d}{dt}\begin{bmatrix}\hat{i}_{L1}\\ \hat{i}_{L2}\\ \hat{v}_{C1}\\ \hat{v}_{C2}\end{bmatrix}=A\begin{bmatrix}\hat{i}_{L1}\\ \hat{i}_{L2}\\ \hat{v}_{C1}\\ \hat{v}_{C2}\end{bmatrix}+B\begin{bmatrix}\hat{v}_d\\ \hat{i}_0\end{bmatrix}+[(A_1-A_2)\begin{bmatrix}I_{L1}\\ I_{L2}\\ V_{C1}\\ V_{C2}\end{bmatrix}+(B_1-B_2)\begin{bmatrix}V_d\\ I_0\end{bmatrix}]\hat{d}+(A\begin{bmatrix}I_{L1}\\ I_{L2}\\ V_{C1}\\ V_{C2}\end{bmatrix}+B\begin{bmatrix}V_d\\ I_0\end{bmatrix}) \tag{7}$$

When the system is stable, the small signal equation of the system is simplified as shown in formula (8).

$$\frac{d}{dt}\begin{bmatrix}\hat{i}_{L1}\\ \hat{i}_{L2}\\ \hat{v}_{C1}\\ \hat{v}_{C2}\end{bmatrix}=A\begin{bmatrix}\hat{i}_{L1}\\ \hat{i}_{L2}\\ \hat{v}_{C1}\\ \hat{v}_{C2}\end{bmatrix}+B\begin{bmatrix}\hat{v}_d\\ \hat{i}_0\end{bmatrix}+[(A_1-A_2)\begin{bmatrix}I_{L1}\\ I_{L2}\\ V_{C1}\\ V_{C2}\end{bmatrix}+(B_1-B_2)\begin{bmatrix}V_d\\ I_0\end{bmatrix}]\hat{d} \tag{8}$$

When $\hat{i}_{L1}=\hat{i}_{L2}=\hat{i}_L$ $v_{C1}=v_{C2}=v_C$
$I_{L1}=I_{L2}=I_L$ $V_{C1}=V_{C2}+V_C$,

Formula (9) can be obtained by Laplace transformation on both sides of formula (8).

$$\begin{cases} si_L(s)=-\dfrac{R+r}{L}i_L(s)-\dfrac{1-2D}{L}v_C(s)+\dfrac{1-D}{L}v_d(s)+\dfrac{(1-D)R}{L}i_0(s)+\dfrac{2V_C-V_d-RI_0}{L}d(s)\\ v_C(s)=\dfrac{1-2D}{C}i_L(s)-\dfrac{1-D}{C}i_0(s)+\dfrac{I_0-2I_L}{C}d(s)\end{cases} \tag{9}$$

Formula (10) can be obtained from formula (9).

$$\begin{aligned}v_C(s)=&\frac{(1-2D)(2V_C-V_d-RI_0)+(I_0-2I_L)(sL+R+r)}{s^2LC+sC(R+r)+(1-2D)^2}d(s)\\ &+\frac{(1-D)(1-2D)}{s^2LC+sC(R+r)+(1-2D)^2}v_d(s)+\frac{(1-D)[(1-2D)R-(sL+R+r)]}{s^2LC+sC(R+r)+(1-2D)^2}i_0(s)\end{aligned} \tag{10}$$

From formula (10), it can be obtained that by controlling the duty cycle D of the direct current, the capacitance-voltage of the Z-network can be controlled, and then the output voltage of the Z-network can be controlled under the non-direct current state, to realize the voltage boost control of the power supply at the DC side. Let i_0(s) and v_d(s) be 0. According to formula (10), the transfer function of the direct duty cycle D and Z-network capacitance-voltage can be obtained as shown in formula (11).

$$G_{Vcd}(s)=\frac{v_c(s)}{d(s)}=\frac{sL(I_0-2I_L)+[(R+r)(I_0-2I_L)+(1-2D)(2V_C-V_d-RI_0)]}{s^2LC+sC(R+r)+(1-2D)^2} \tag{11}$$

3. Controller design and closed-loop simulation of Z-source inverter

The control of the Z-source inverter includes the step-up control of the Z-

network and the current control of the inverter [7, 12]. Because there is a certain proportion between the capacitance-voltage of the Z-network and the peak voltage of the H-bridge, the stable capacitance voltage has a positive role in promoting the stability of the peak voltage of the H-bridge. The design of the Z-source network boost control structure is shown in Fig. 2.

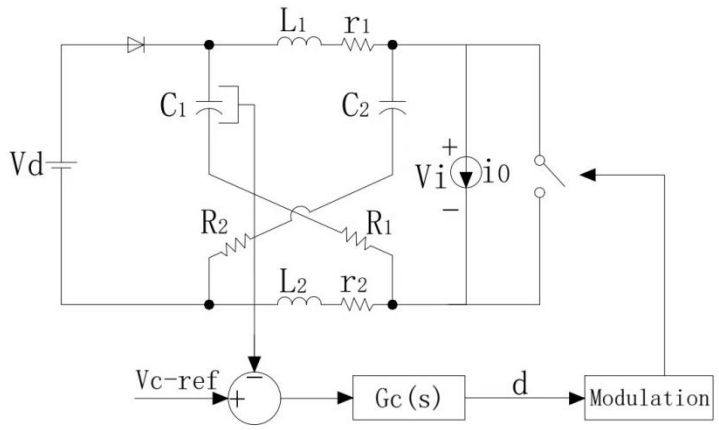

Fig. 2. Z-source network boost control structure chart

The difference between the standard value of capacitance-voltage $V_{c\text{-}ref}$ and the actual value of capacitance-voltage V_c is taken as the error signal, which is sent to the controller whose transfer function is $G_c(s)$ as the input. The duty cycle of the output shoot-through of the transfer function is d. d is sent to the modulator for modulation, and the modulated signal controls the shoot-through of the H-bridge. Since formula (11) obtains the transfer function of Z-network from direct duty ratio d to capacitor voltage, the above control structure can be represented by the block diagram as shown in Fig. 3.

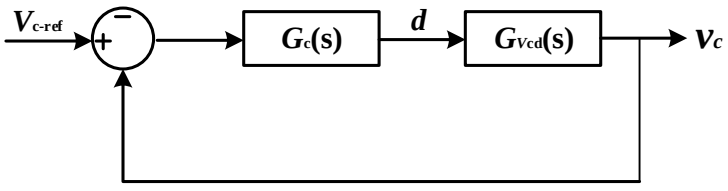

Fig. 3. Z-network boost control block diagram

According to the engineering design requirements, the circuit device parameters are selected as follows: C=1000μF, L=3mH, r=0.3Ω, R=0.05Ω, V_d=510V, D=0.35, I_0=15A. According to equation (6), I_L=32.5A. Taking the above data into equation (11), the transfer function is obtained as follows:

$$G_{Vcd}(s)=\frac{-0.15s+450}{3\times10^{-6}s^2+3.5\times10^{-4}s+0.09}$$

It can be seen from the Bode diagram of the transfer function that the Z-network is an open-loop structure. The amplitude margin of the system is negative (Gm = -52.6db), and the phase angle margin is also negative (Pm = -86.4deg), so the system is unstable.

The gain of open-loop transfer function $G_{Vcd}(s)$ is adjusted. The error coefficient of the unit step is 20. The gain coefficient K, $K=\frac{20}{\lim\limits_{s\to0}G_{Vcd}(s)}=0.004$, is obtained. After adjusting the gain, the open-loop transfer function is as follows:

$$G_0(s)=\frac{-6\times10^{-4}s+1.8}{3\times10^{-6}s^2+3.5\times10^{-4}s+0.09}$$

According to the Bode diagram of the open-loop transfer function of the z-network, the amplitude margin of the system is negative (Gm = -4.68db), and the phase margin is also negative (Pm = -6.31deg). After adjusting the gain, the system is still unstable, so a series leading correction link is needed to increase its amplitude and phase margin.

If the parameters of the system can not meet the requirements of all performance simultaneously, some devices can be added to the system to improve the performance. The series advance correction is to connect the correction device $G_c(s)$ in series in the forward channel of the system. The design of the series correction device is dependent on the transfer function $G_0(s)$ of the inherent part and the performance requirements of the system.

The series advance correction is to increase the phase angle stability margin of the system by utilizing the phase advance characteristic of the correction device, and increase the crossing frequency of the system by using the positive slope of the amplitude-frequency characteristic curve of the correction device, so that we can improve the stability and rapidity of the system. Therefore, the maximum design advance phase angle appears at the new crossing frequency of the system [13].

The transfer function of the series leading correction link is: $G_c(s)=\frac{aTs+1}{Ts+1}$

If the compensation value is 55 degrees, there are: $a=\frac{1+\sin(55^\circ)}{1-\sin(55^\circ)}=10$

To make the best use of the leading phase angle, the cut-off frequency after setting correction has the following relations:

$$10\lg|G_0(j\omega_c)|=-10\lg a$$

It can be seen that, when the system amplitude is $-10\lg a=-10dB$, the cut-off frequency is: $\omega_c=1.46\times10^{-3}rad/s$, and there is: $T=\frac{1}{\omega_c\sqrt{a}}=2.17\times10^{-4}$

According to the above derivation, the transfer function of the advance correction link can be obtained as follows: $G_c(s)=\frac{2..17\times10^{-3}s+1}{2..17\times10^{-4}s+1}$

The frequency domain characteristics of the system after series lead correction is shown in Fig.. 4.

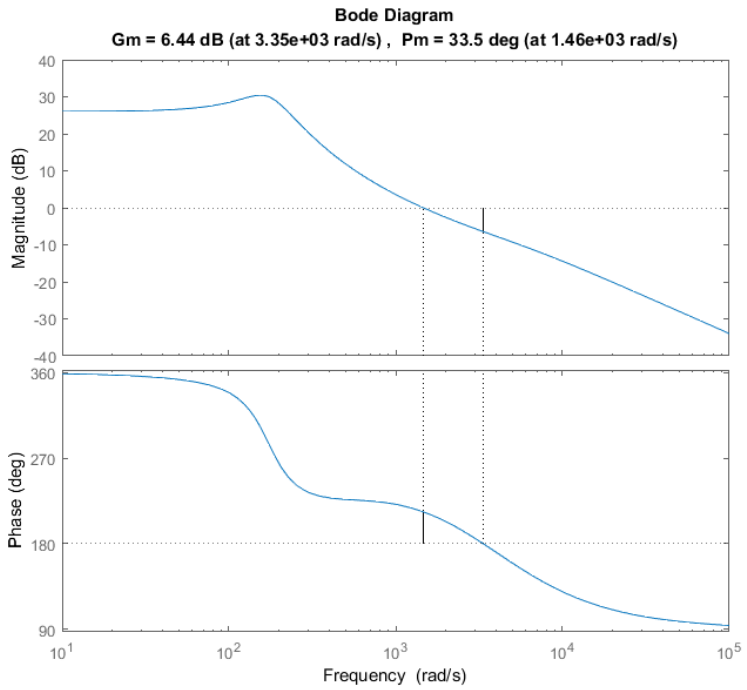

Fig. 4. Frequency domain characteristics of advanced correction system

It can be seen from Fig. 4 that the amplitude-frequency and phase-frequency characteristics of the system are both positive, and the amplitude margin is positive (Gm = 6.44db), while the phase angle margin Pm reaches 35.5 degrees, at this time the system is stable.

It can be seen from the above analysis that the series lead correction has the following characteristics:

(1) The series lead correction is mainly aimed at the IF section of the system frequency characteristic, so that the IF section slope of the amplitude-frequency characteristic curve after correction is - 20dB/Dec, and there is enough phase margin.

(2) The series leading correction will increase the system's passing frequency, which shows that the frequency band of the system after correction is wider, the instantaneous response speed is faster, but the system's ability to resist high-frequency interference is worse.

(3) It is difficult to improve the low-frequency characteristics of the original

system by series lead correction. If the low-frequency section is to be moved up by the method of providing gain, the stability of the system will be poor and the ability to resist high-frequency noise will be weakened because the whole amplitude-frequency characteristic curve is moved up [14-15].

The simulation model of the Z-source inverter circuit is built, and the simulation diagram of SimPowerSystems is shown in Fig. 5.

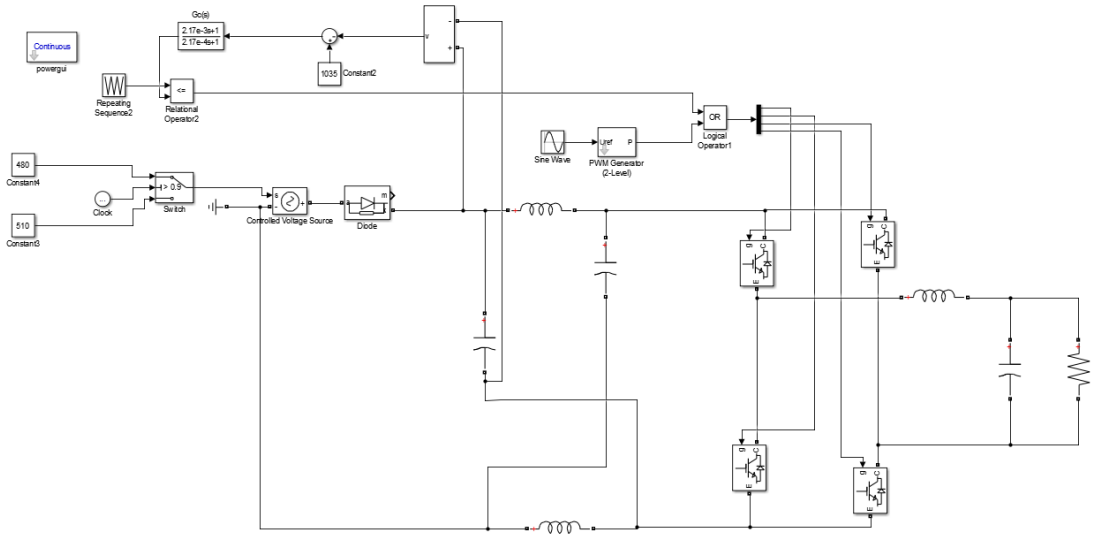

Fig. 5. Simulation Model of Z-source Inverter Circuit

The closed-loop simulation of the Z-source inverter circuit is carried out by using the designed controller, and the simulation results as shown in Fig. 6 are obtained.

In the figure, Vac represents the output voltage at the AC side, Vdc-link represents the voltage at both ends of the inverter bridge, Vc represents the voltage of the capacitor in the Z-source network, and Vd represents the input DC voltage.

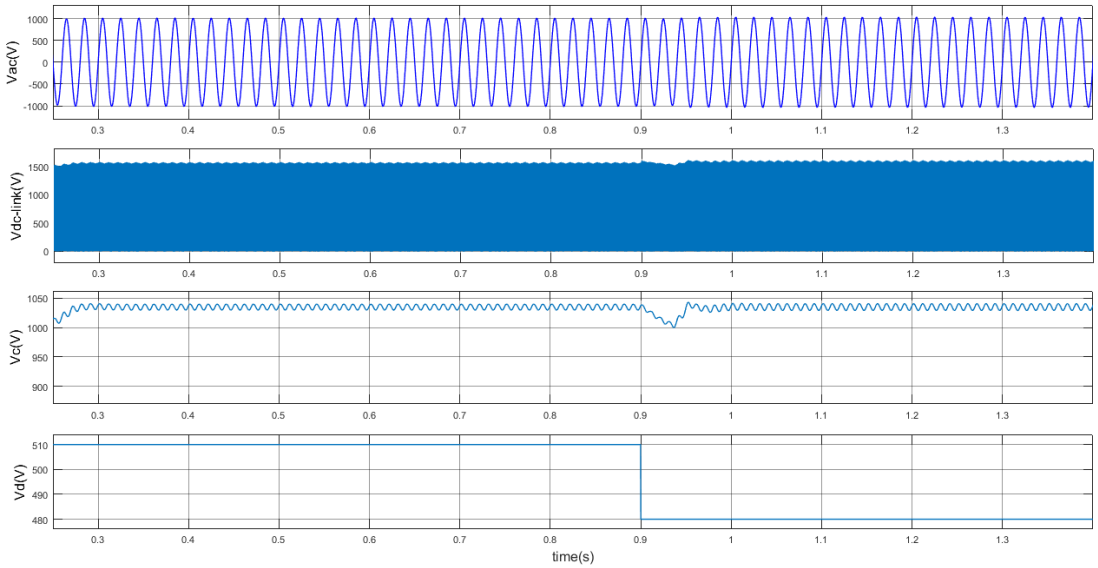

Fig. 6. Simulation results of Z-source Inverters

According to the simulation results in Fig. 6, when the input voltage V_d at the DC side drops from 510V to 480V in 0.9s, it hardly affects the final output voltage of the Z-source inverter. The closed-loop system has strong anti-interference ability and can provide a stable and appropriate voltage for the later-stage circuit.

Different from the traditional inverter transformer combination inverter boost structure, the Z-source inverter can raise the DC side voltage and the output AC voltage to a larger level by adjusting its direct duty cycle D, and reach the 1000V required by the previous level of voltage regulation. To get a higher AC voltage, the traditional method is to realize the inverter boost to the required voltage through the inverter and transformer. The advantage of a Z-source inverter is that when the input voltage fluctuates, it can still control the output voltage to be stable at the required level. Simultaneously, because the impedance network of the Z-source inverter has inductance when the electromagnetic interference causes the inverter bridge arm to shoot through, the current through the bridge arm will not suddenly increase and the bridge arm will be burnt out. Compared with the two-stage converter, it can greatly reduce energy consumption.

4. Experimental test and analysis

The control signal is sent to the controller and the duty cycle is output. Then, the duty cycle is sent to the modulator to control the H-bridge by the driving circuit. Consequently, the output voltage of the Z-network in anon-shoot-through state is controlled by controlling the capacitor voltage of the Z-network.

The continuous adjustment of the duty cycle can be realized by the adjustable resistance technology of the SG3525 integrated PWM chip, and its adjustment range is 0% - 50%, which meets the corresponding technical requirements. The out A signal and out B signal of SG3525 are sent to the M57962 chip to generate the control signal (peak pulse) required by the H-bridge circuit. The control signal is connected to the G pole (grid G) of the IGBT drive circuit to control the IGBT circuit on or off.

The driving power of the filtered IGBT circuit signal fails to meet the conduction conditions of the IGBT module, so the driving circuit needs to amplify the power. The single transistor high-power IGBT module is used to drive M57962 in this paper. M57962 is a thick-film integrated circuit designed by Mitsubishi Electric to drive the IGBT module. It integrates a 2500V Isolated High-voltage Optocoupler, overcurrent protection current, and overcurrent protection terminal, and has the characteristic of short-circuit protection.

Protel DXP software is used to design the circuit, and the driving circuit diagram is shown in Fig. 7.

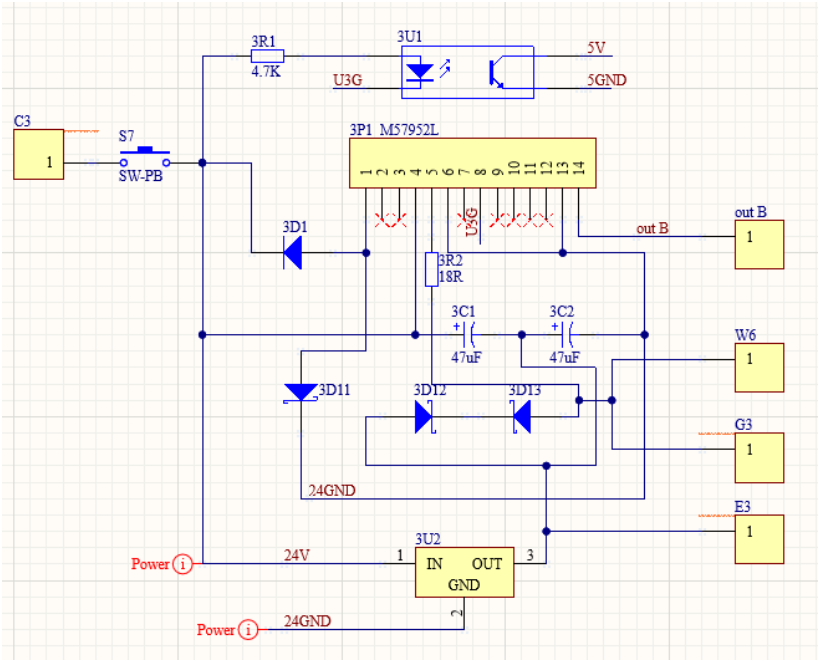

Fig. 7. Driving Circuit Diagram

Pin 14 of M57962L is connected to PWM signal input (generated by out A of SG3525 module) to form the front stage, and G1, C1, and E1 in the figure are connected to grid G, collector C, and emitter E of IGBT tube respectively. The pin 14 signal and G1 signal are measured by the oscilloscope, and the results are shown in Fig. 8.

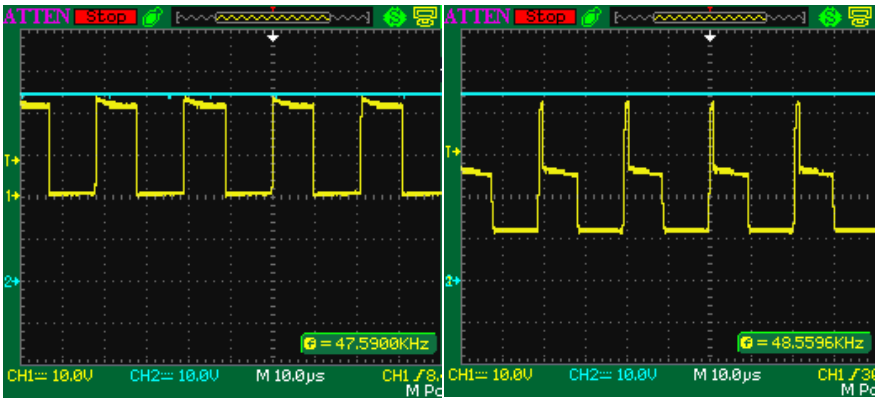

a) Pin 14 signal input waveform b) G1 signal output waveform

Fig. 8. Driving circuit waveform

As shown in Fig. 8, the PWMA frequency waveform (f = 47.59KHz, D = 50%) of SG3525 is connected to pin 14 of M57962L, and the signal output waveform (f = 48.56KHz, D = 50%) of G1 is obtained through the driving circuit. The result shows that the peak pulse used to drive the IGBT tube is generated after the signal passes through the driving circuit, but the frequency and the duty cycle remain almost unchanged. The test signal meets the expectation and can control the on and of in the IGBT driving circuit. When adjusting the duty cycle to the state of f = 50KHz and D = 0%, the load does not work.

5. Conclusion

In this paper, we study the Z-source inverter controller using the state space average method, and the conclusions are as follows:

(1) The average state equation and steady-state equation of the system are both obtained by Laplace transform, and the transfer function of direct duty cycle D and Z-network capacitance voltage is obtained. The control structure is analyzed and the gain of the transfer function is adjusted. A series leading correction link is added. The results show that the amplitude margin Gm increased from -52.6db to 6.44db, and the phase margin Pm is increased from -86.4deg to 33.5deg. The performance of the controller is greatly optimized and the system is stable.

(2) The simulation model of the Z-source inverter circuit is built by SimPowerSystems. The results show that when the input voltage V_d of the DC side drops from 510V to 480V in 0.9s, the final output voltage of the Z-source inverter nearly remains constant. The closed-loop system has strong anti-interference ability and can boost voltage and prevent the bridge arm from burning directly. It can provide a stable and appropriate voltage for the later circuit.

(3) The control circuit of the Z-source inverter is designed, and the direct duty cycle D and M57962 driving circuits are tested in this paper. The experimental

results show that D can be adjustable continuously from 0 to 45%, and can achieve 1-10 times of voltage boost. In addition, the control circuit can work in a shoot-through state, and control H-bridge. What's more, the peak pulse of the driving circuit meets the requirements.

Funding

This research was funded by No. 2023CJRHJD002 and No. 2023ZDZX2051.

REFERENCES

[1] *F. Z. Peng*, "Z-source inverter", IEEE Trans. Ind. Appl., vol. 39, no. 2, 2003, pp. 504–510.DOI: 10.1109/TIA.2003.808920

[2] *Z. Rymarski, K. Bernacki and L. Dyga*, "Controlled Energy Flow in Z-Source Inverters", Energies, vol. 14, no. 21, 2021, pp.7272.DOI:10.3390/en14217272

[3] *V. K. Bussa, A. Ahmad, R. K. Singh and R. Mahanty*, "Single-phase high-voltage gain switched LC Z-source inverters", IET Power Electronics, vol. 11, no. 5, 2018, pp. 796–807. DOI:10.1049/iet-pel.2017.0634

[4] *A. A. Hossameldin, A. K. Abdelsalam, A. A. Ibrahim and B. W. Williams*, "Enhanced Performance Modified Discontinuous PWM Technique for Three-Phase Z-Source Inverter", Energies, vol. 13, no. 3, 2020, pp. 578. DOI: 10.3390/en13030578

[5] *M. Mohammadi, J. S. Moghani and J. Milimonfared*, "A Novel Dual Switching Frequency Modulation for Z-Source and Quasi-Z-Source Inverters", IEEE Transactions on Industrial Electronics, vol. 65, no. 6, 2018, pp. 5167-5176. DOI: 10.1109/tie.2017.2784346

[6] *A. Abdelhakim, P. Davari, F. Blaabjerg and P. Mattavelli*, "Switching Loss Reduction in the Three-Phase Quasi-Z-Source Inverters Utilizing Modified Space Vector Modulation Strategies", IEEE Transactions on Power Electronics, vol. 33, no. 5, 2018, pp. 4045-4060. DOI: 10.1109/tpel.2017.2721402

[7] *Y. P. Siwakoti, F. Z. Peng, F. Blaabjerg, P. C. Loh andG. E. Town*, "Impedance-Source Networks for Electric PowerConversion Part I: A Topological Review", IEEE Transactionson Power Electronics, vol. 30, no. 2, 2015, pp. 699-716.DOI: 10.1109/tpel.2014.2313746

[8] *Y. P. Siwakoti, F. Z. Peng, F. Blaabjerg, P. C. Loh,G. E. Town andS. Yang*, "Impedance-Source Networks for Electric Power Conversion Part II: Review of Control and Modulation Techniques", IEEE Transactions on Power Electronics, vol. 30, no. 4, 2015, pp. 1887-1906.DOI:10.1109/tpel.2014.2329859

[9] *C. Roncero-Clemente, O. Husev, T. Jalakas, E. Romero-Cadaval, J. Zakis and V. Miñambres-Marcos*, "PWM for single phase 3L Z/qZ-source inverter with balanced power losses", ElektronikaIr Elektrotechnika, vol. 20, 2014, pp. 71-76.DOI: 10.5755/j01.eee.20.6.7270

[10] *O. Husev, C. Roncero-Clemente, E. Romero-Cadaval, D. Vinnikov and S. Stepenko*, "Single phasethree-level neutral-point-clamped quasi-Z-source inverter", IET Power Electronics, vol. 8, no. 1, 2015, pp. 1-10.DOI: 10.1049/iet-pel.2013.0904

[11] *B. Barathy, A. Kavitha andT. Viswanathan*, "Effective space vector modulation switching sequence for three phase Z source inverters", IET Power Electronics, vol. 7, no. 11, 2014, pp. 2695-2703.DOI: 10.1049/iet-pel.2013.0903

[12] *Y. Liu, B. Ge and H. Abu-Rub*, "Theoretical and experimental evaluation of four space-vector

modulations applied to quasi-Z-source inverters", IET Power Electronics, vol. 6, no. 7, 2013, pp. 1257-1269.DOI: 10.1049/iet-pel.2012.0681

[13] *M. R. Banaei and E. Salary*, "New multilevel inverter with reduction of switches and gate driver", Energy Conversion and Management, vol. 52, no. 2, 2011, pp. 1129-1136.DOI: 10.1016/j.enconman.2010.09.007

[14] *K. El-Naggar and T. H. Abdelhamid*, "Selective harmonic elimination of new family of multilevel inverters using genetic algorithms", Energy Conversion and Management, vol. 49, no. 1, 2008, pp. 89-95.DOI: 10.1016/j.enconman.2007.05.014

[15] *E. Babaei and S. H. Hosseini*, "New cascaded multilevel inverter topology with minimum number of switches", Energy Conversion and Management, vol. 50, no. 11, 2009, pp. 2761-2767.DOI: 10.1016/j.enconman.2009.06.032